A note on the power potential of tidal currents in channels.

Citation for published version:
Draper, S, Adcock, TAA, Borthwick, A & Houlsby, GT 2014, 'A note on the power potential of tidal currents in channels.', *International Journal of Marine Energy*, vol. 6, pp. 1-17.
https://doi.org/10.1016/j.ijome.2014.05.001

Digital Object Identifier (DOI):
10.1016/j.ijome.2014.05.001

Link:
Link to publication record in Edinburgh Research Explorer

Document Version:
Early version, also known as pre-print

Published In:
International Journal of Marine Energy

Abstract

This paper presents a set of three simple one-equation formulas that can be used for rapid initial resource assessment of the tidal power potential of fast moving currents in large straits and small tidal channels (as may exist close to isolated communities). The three formulas enhance previous published theoretical estimates and are consistent with each other in that any one of them can be used depending on which two of the following three input parameters are known: (i) the variation in water level at either end of the channel (or just at the ocean end for a channel connected to an enclosed bay); (ii) the peak undisturbed natural flow rate through the channel; or (iii) the approximate channel geometry and seabed drag coefficient. The formulas are derived using an electrical analogy of the dynamics of flow through a channel. Example calculations are given and the results compare favourably with previous estimates of power potential by alternative theoretical formulas and detailed numerical models.

Keywords: tidal energy, tidal power, tidal resource assessment, tidal channel.

Nomenclature

a_0	Amplitude of the difference in free surface elevation across a channel associated with the dominant tidal constituent [m]
$a_{0,j}$	Amplitude of the difference in free surface elevation across a channel associated with the additional tidal constituents [m]
a_1	Amplitude of the free surface elevation in the large water body that connects to a channel and a smaller enclosed bay. Elevation associated with dominant tidal constituent [m]
$a_{1,j}$	Amplitude of the free surface elevation in the large water body that connects to a channel and a smaller enclosed bay. Elevation associated with additional tidal constituents [m]
c	Parameter defining geometry of tidal channel ($c = \int_0^l A^{-1}\, dx$) [m^{-1}]
g	Acceleration due to gravity [m/s^2]
h	Mean water depth as a function of position along a tidal channel [m]
i	Complex number √(-1) [-]
l	Length of tidal channel [m]
t	Time [s]
x	Distance along channel [m]
A_e, l_e, h_e	Effective geometric parameters which may be estimated for a tidal channel [m^2,m,m]
A	Cross-sectional area as a function of position along tidal channel [m^2]
C	Capacitance in an equivalent circuit [NA]
C_d	Drag coefficient parameterising seabed friction in tidal channel [-]
I	Current in an analogous electrical circuit [NA]
L	Inductance in an analogous electrical circuit [NA]
$\bar{P}$	Power extracted by tidal turbines, averaged over a tidal cycle [Watts]
$\bar{P}_{max}$	Maximum power extracted by tidal turbines, averaged over a tidal cycle [Watts]
R	Resistance in an analogous electrical circuit [NA]
S	Surface area of enclosed bay [m^2]
$S_{channel}$	Surface area of a channel connecting to an enclosed bay [m^2]
T	Period of tidal wave (=$2\pi/\omega$) [s]
V	Voltage in an analogous electrical circuit [NA]
Q	Flow rate through the channel [m^3/s]
$Q_{0,max}$	Maximum flow rate associated with the dominant tidal constituent before turbines are installed in channel [m^3/s]
$Q_{0,max,j}$	Maximum flow rate associated with additional tidal constituents before turbines are installed in channel [m^3/s]
$Q_{0,max,S/N}$	Maximum flow rate before turbines are installed at Spring tidal and Neap tide, respectively [m^3/s]
Z	Impedance in an analogous electrical circuit [NA]

β	Non-dimensional term which defines geometry of a channel connected to an enclosed bay [-]
γ	Non-dimensional term which parameterises the effects of resistance and impendence on the maximum power extraction [-]
δ_t	Parameter defining resistance due to tidal turbines [m^{-4}]
δ	Parameter defining resistance due to bed friction in tidal channel [m^{-4}]
λ	Non-dimensional term which parameterises natural bed friction, geometry and tidal amplitude for a tidal channel connecting two large bodies of water [-]
λ_1	Non-dimensional term which parameterises natural bed friction, geometry and tidal amplitude for a tidal channel connected to an enclosed bay [-]
ξ	Free surface elevation above still water level [m]
ξ_0	Free surface elevation difference across channel [m]
ξ_1	Free surface elevation in the large water body that connects to a channel and a smaller enclosed bay [m]
ρ	Density of seawater [kg/m^3]
σ_1	Parameter defining tidal channel geometry, angular frequency and seabed friction defined by Equation (23) [rad/ms]
σ_2	Parameter defining tidal channel geometry, angular frequency and seabed friction defined by Equation (23) [m^{-4}]
ω	Angular frequency of tidal wave (=$2\pi/\omega$) [s]

1.0 Introduction

Resource assessments of tidal stream power generation were first undertaken about 5-10 years ago, with most attention paid to the sites off the United Kingdom (e.g. Black and Veatch 2005) and North America (e.g. Triton Consultants, 2006). However, these assessments used the undisturbed kinetic flux in estimating the power potential of tidal currents in channels. It has since been shown that the kinetic flux is not related in any general way to the power that can be generated in a tidal channel or the change in flow through a channel that may be experienced when tidal turbines are deployed (Garrett and Cummins, 2005; hereafter GC05).

In order to obtain a more correct assessment of the power potential of tidal currents in channels GC05 introduced a theoretical model of flow through a tidal channel which allowed for the effect of the presence of the turbines on the flow (see Section 2 for further details). GC05's model considered a tidal channel with slowly varying geometry connecting two large basins of water and has been shown to give estimates that agree remarkably well with depth-averaged numerical simulations (see, for example, Sutherland *et al.* 2007 and Draper *et al.* 2013a). A subsequent extension of the model has been made to predict the tidal power potential of a channel connected to an enclosed bay (see Blanchfield *et al.*, 2008; hereafter B08), and an approximate analytical solution to this extended model has been shown to compare well with depth-averaged numerical simulations (Karsten *et al.* 2008).

A convenient aspect of the theoretical models of GC05 and the extended model of B08 is that they lead to one-equation formulas that can be used to estimate the power potential of a tidal channel. These one-equation formulas are easy to use in practice provided estimates or measurements are available of the peak undisturbed flow rate through the channel (i.e. the peak flow rate prior to the installation of tidal turbines) and the dynamic head driving flow through the channel (i.e. the amplitude in the water level difference between each end of the channel, or the amplitude of water level variation in the larger water body for a channel connected to an enclosed bay). In certain cases however, Vennell (2011) has pointed out that the dynamic head parameter may be difficult to estimate in practice because either it is too small to measure accurately for a short channel or because measurements are not available of the water level either side of the channel. To circumvent this problem Vennell (2011) developed an algorithm to calculate the power potential of a tidal channel from estimates of the undisturbed peak flow rate and the channel geometry combined with a seabed drag coefficient, as opposed to the dynamic head.

In this paper we expand on GC05's and B08's solutions in a different way to that of Vennell (2011) and derive a set of three simple one-equation formulas that can be used to estimate the power potential of tidal currents in a channel connecting two large water bodies (referred to herein as a Type 1 channel) and a similar set of three one-equation formulas for a channel connected to an enclosed bay (referred to herein as a Type 2 channel). The three formulas for each type of channel are compatible in that any one of them can be used depending on which two of the following three parameters are known (or are easiest to estimate): (i) the amplitude of water level difference across the channel (or simply the amplitude of water level variation in the larger water body for a Type 2 channel); (ii) the peak natural flow rate through the channel; or (iii) the approximate channel geometry and seabed drag coefficient.

With reference to previous work, for each type of channel the first of the three simple one-equation formulas presented herein, which can be used if only (i) and (ii) are known, is exactly that given by GC05 for Type 1 channels and B08 for Type 2 channels. In contrast the second one-equation formula derived for each type of channel, which can be used if only (ii) and (iii) are known, was not given by GC05 or BC08 and is distinct from the algorithm given by Vennell (2011), although it gives similar results. Finally, the third one-equation formula derived herein for each type of channel, which can be used if only (i) and (iii) are known, was not given by either GC05 or Vennell (2011). This formula is particularly useful when only tidal elevations and nautical charts (without tidal streams, but with bathymetry) are available. This can often be the case in isolated locations where scoping studies of tidal stream power may be required.

The remainder of this paper is set out as follows. First we review the theoretical model of GC05 and the extension of B08 to describe flow through both types of channel. A simple electrical analogy is then used to interpret these theoretical models, from which one-equation formulas are constructed to estimate the power potential. Example calculations are presented, illustrating typical applications of the formulas. The paper concludes by discussing the implications of using the simple formulas to assess which tidal channels are potentially the most attractive for tidal stream power generation.

It should be noted that this paper is concerned with estimating the power that can be extracted from a tidal channel, not the power that may be available to a given number and arrangement of tidal turbines. Vennell (2010) makes this distinction clearly for the first type of channel discussed herein. Vennell's analysis is important in assessing which channels are most attractive for tidal power generation, as discussed further in the final section of this paper.

2.0 Theoretical models for tidal channels

2.1 *Channel connecting two large bodies of water (Type 1 Channel)*

GC05 introduced a theoretical model to describe the flow of water through a tidal channel of smoothly varying geometry (see Figure 1a). To model flow through a channel they start from the one-dimensional shallow water approximation to the momentum equation:

$$\rho\frac{\partial}{\partial t}\left(\frac{Q}{A}\right)+\frac{\rho Q}{A}\frac{\partial}{\partial x}\left(\frac{Q}{A}\right)+\rho g\frac{\partial \xi}{\partial x}=-\rho\left(\frac{C_d}{hA^2}+\delta_t\right)Q|Q|, \tag{1}$$

where $Q(x,t)$ is the one-dimensional flow rate through the channel, $\xi(x,t)$ is the free surface elevation above mean water level, ρ is water density, g is acceleration due to gravity, $A$is the cross-sectional area of the channel, h is the average water depth at any point along the channel, C_d is a drag coefficient parameterising background friction in the channel, and δ_t is a resistance introduced to represent tidal devices placed across the width of the channel. The definition of this resistance implies that the power extracted from the channel by tidal devices, averaged over a tidal period T, is $\bar{P} = (\rho \int_0^T \delta_t |Q|^3 \, dt)/T$.

To simplify Equation (1) GC05 made some important assumptions. Firstly, they reasoned that most tidal channels are short compared to a characteristic tidal wavelength so that the flow rate Q is approximately the same everywhere along the channel (i.e. depth averaged velocities within the channel are non-divergent; see also Vennell (1998)). They also assumed that variations in the wet cross-sectional area of the channel would be small over the tidal cycle, so that Equation (1) could be integrated along the channel length, l, and rearranged to give:

$$\rho g \xi_a = \rho c \frac{dQ}{dt} + \rho \delta_t Q|Q| + \rho \left(\frac{1}{2A_{end}^2} - \frac{1}{2A_{start}^2} + \int_0^l \frac{C_d}{hA^2} dx \right) Q|Q|, \tag{2}$$

where $c = \int_0^l A^{-1} \, dx$, $\xi_0 = \xi(0,t) - \xi(l,t)$ is the time-varying free surface elevation difference either side of the channel, and the parameters A_{start} and A_{end} define the cross-sectional areas at the exit and entrance of the channel, respectively. These latter two parameters are often difficult to define and their difference can be small for many tidal channels. In this paper we will ignore these parameters (this appears to be justified; see example calculations in Section 4). Flow through the channel is therefore given by:

$$\rho g \xi_0 = \rho c \frac{dQ}{dt} + (\rho \delta_t |Q| + \rho \delta |Q|) Q, \tag{3}$$

where δ defines the integral in Equation (2).

Next, GC05 assume that the time varying water level difference (or dynamic head) denoted by ξ_0 in Equation (3) does not change in amplitude when turbines are added to the channel. This assumption is likely to hold when the surrounding water bodies feeding the channel are large in lateral extent and depth. GC05 also assume that the dynamic head can be represented by $\xi_0 = a_0 \cos(\omega t)$, where ω (=$2\pi/T$) is the frequency of the principal tidal constituent (which is assumed to dominate other constituents) and a_0 is the amplitude in elevation difference across the channel.

Adopting each of these assumptions Equation (3) can be solved directly for various channel geometries (defined by c and δ), and the average power extracted by tidal turbines $\bar{P}$ can be calculated for different values of δ_t.

In solving Equation (3) GC05 show that for each channel geometry there is a trade-off between increasing the drag from turbines to generate more power and having so much drag that the flow through the channel reduces substantially thus limiting power extraction. This implies that there is an optimum amount of power extraction, which GC05 show can be estimated for any channel geometry using the equation:

$$\overline{P}_{max} = \gamma_{GC} \rho g a_0 Q_{0,max}, \tag{4}$$

where $\overline{P}_{max}$ is the power potential of the tidal channel (i.e. the maximum power that can be extracted, averaged over a tidal period), $Q_{0,max}$ is the maximum flow rate through the channel prior to the introduction of tidal turbines and γ_{GC} is a multiplier that depends on the dynamic balance in the channel, as indicated by the phase lag of the flow rate behind the driving head (GC05). Conveniently, however, GC05 show that the dependence of this multiplier on the dynamic balance is weak. Consequently adopting the fixed value of γ_{GC} =0.22 gives an approximate solution that is accurate to within 10% of the theoretical model result for any dynamic balance.

As noted earlier, Equation (4) has been used by Sutherland *et al.* (2007) and Draper *et al.* (2013a) to provide remarkably good predictions of the power potential of tidal currents when compared with results from detailed numerical models. If γ_{GC} is taken to be 0.22 it is now easy to see, as noted in the Introduction, that the formula can be applied in practice provided the undisturbed peak flow rate $Q_{0,max}$ can be measured from, for example, ADCP field measurements or a numerical model (without tidal turbines included), together with the amplitude a_0. If the water level variation due to the dominant tidal constituent at either end of the channel is $\xi_X = a_X \cos(\omega t + \phi_X)$ and $\xi_Y = a_Y \cos(\omega t + \phi_Y)$, respectively, then this amplitude is simply $a_0 = (a_X^2 + a_Y^2 - 2a_X a_Y \cos(\phi_Y - \phi_X))^{1/2}$.

2.2 *Channel connected to an enclosed bay (Type* 2 *Channel)*

B08 extended the model of GC05 (and the earlier work of Garrett and Cummins, 2004) to a tidal channel connected to an enclosed bay (see Figure 2a). Blanchfield et al.'s theoretical model of flow in a tidal channel is identical to Equation (3), except that the difference in water level across the channel is decomposed into:

$$\xi_0 = \xi_1 - \xi_b, \tag{5}$$

where ξ_1 defines the time-varying water surface elevation in the large body of water and ξ_b is the time-varying elevation above mean water level in the enclosed bay. ξ_1 is assumed to remain unchanged with the addition of turbines, whereas ξ_b is linked to the flow rate through the channel and can therefore vary with the addition of turbines. Invoking conservation of volume, the bay elevation satisfies

$$S\frac{d\xi_b}{dt} = Q \quad \text{or} \quad \xi_b(t) = \frac{1}{S}\int Q(t)dt \tag{6}$$

where S is the surface area of the enclosed bay, which is assumed to remain constant as the water level in the bay rises and falls. Combining Equation (3) and Equation (6), the flow through a channel connected to an enclosed bay is modelled by B08 as:

$$\rho g \xi_1 = \rho c \frac{\partial Q}{\partial t} + (\rho\delta_t + \rho\delta)|Q|Q + \frac{\rho g}{S}\int Q(t)dt, \tag{7}$$

For various channel and bay geometries (defined by S, c and δ) and for a sinusoidal driving water level in the large body of water given by $\xi_1 = a_1 \cos(\omega t)$, B08 solve this equation and determine that the maximum power extracted by turbines can be written as:

$$\bar{P}_{max} = \gamma_B \rho g a_1 Q_{0,max}, \tag{8}$$

where γ_B is a new multiplier that depends on the dynamic balance in the channel and the geometry of the bay relative to the channel (see B08). However, the multiplier is not very sensitive to changes in these parameters and may also be chosen as 0.22 to give a reasonable approximation in all cases.

Despite their similarity, Equation (8) is slightly different to Equation (4). The subtle difference between both equations is that the amplitude in Equation (8) is not the amplitude of elevation difference across the channel, but instead the amplitude of water level variations in the large body of water. However, as expected, in the limit of a very large enclosed bay Equation (8) is identical to Equation (4) provided that the enclosed bay does not oscillate independently of the large water body (B08).

3.0 Electrical interpretation of theoretical models

Equation (3) and Equation (7) describe the basic dynamics of flow through both types of tidal channel. We now interpret these models using an electrical analogy, following the work of Cummins (2013) and Draper *et al.* (2013b). This interpretation will prove useful later in deriving alternative one-equation formulas to predict $\bar{P}_{max}$.

To introduce the analogy we compare Equation (3) and Equation (7) with:

$$V = L\frac{dI}{dt} + RI + \frac{1}{C}\int I\,dt, \tag{9}$$

which describes the time varying current I in an electric circuit with inductance L, resistance R, capacitance C and driving voltage V. Adopting $Q \equiv I$, a direct comparison with Equation (3) and Equation (7) suggests that $\rho g \xi_0$ and $\rho g \xi_1$ can be interpreted as driving voltages, whereas the mass of water passing through the channel leads to an inductance $L = \rho c$, and the natural drag and drag due to tidal devices can be represented by non-linear resistors $R = \rho\delta|Q|$ and $R_t = \rho\delta_t|Q|$. Finally, the enclosed bay (applicable for the second type of channel) introduces a capacitance $C = S/\rho g$. The tidal channels are thus equivalent to the electric circuits shown in Figure 1b and Figure 2b.

Given that ξ_0 and ξ_1 are assumed to be fixed in the theoretical models, respectively, the voltage in both circuits is fixed and so the addition of turbines simply acts to increase R_t and hence the effective impedance in the circuit. In turn this must reduce the current flowing through the circuit and so, as outlined by Cummins (2013) and Draper *et al.* (2013b), it is therefore easy to see that there must be an optimum value of power extraction.

To calculate this optimum value, the power dissipated in the resistor representing the tidal turbines should be maximised. Based on elementary electric circuit theory this can be achieved via impedance matching if all resistors are linear. For example, assuming a single tidal constituent (i.e. $V \equiv a_0 e^{i\omega t}$ or $V \equiv a_1 e^{i\omega t}$), and initially ignoring the non-linearity of the resistors, then the optimum tidal device resistance is simply $R_{t,opt} = |Z| = ((\omega L)^2(1-\beta)^2 + R^2)^{1/2}$, where $Z = i\omega L - i/(\omega C) + R$ is the natural impedance of the channel, and

$$\beta = \frac{1}{\omega^2 CL} = \frac{g}{\omega^2 Sc}. \tag{10}$$

The optimum power (averaged over a tidal cycle) can subsequently be written as (see also Cummins (2013) and Draper *et al.* (2013b)):

$$\overline{P}_{max} = \frac{1}{4}\left(\frac{1}{1+R/|Z|}\right)|V||I_0|, \tag{11}$$

where $|I_0|$ is the peak current before a resistance due to tidal devices is introduced (i.e. $|I_0| = Q_{0,max}$). This result can be rewritten for channels connecting two large water bodies as (i.e. Type 1 channels):

$$\overline{P}_{max} = \frac{1}{4}\left(\frac{1}{1+R/|Z|}\right)\rho g a_0 Q_{0,max}\,, \tag{12}$$

and for a channel connected to an enclosed bay it can be written as (i.e. Type 2 channels):

$$\overline{P}_{max} = \frac{1}{4}\left(\frac{1}{1+R/|Z|}\right)\rho g a_1 Q_{0,max}. \tag{13}$$

In (12) it is assumed that $\beta = 0$ in Z.

Although Equations (12) and (13) are derived for linear resistances, their form is strikingly similar to the non-linear Equations (4) and (8). The only difference is the multiplier on the product of the undisturbed flow rate and dynamic pressure. In the linear case this multiplier can be seen to vary between 0.125 to 0.25 for a channel with no natural drag (i.e. $R/|Z| \rightarrow 0$) and a channel with drag-dominated impedance ($R/|Z| \rightarrow 1$). Alternatively, for the non-linear result in Equation (4) GC05 show that the multiplier γ_{GC} depends on just a single parameter $\lambda = g a_0 \delta/(c\omega)^2$, which also describes the proportion of the channel's impedance due to drag (but also includes the dynamic head because of the non-linear dependence on flow rate). This multiplier limits from $\gamma_{GC} = 0.24$ for a channel with no natural drag to $\gamma = 0.21$ for a channel that is drag-dominated (see also Figure 3). Thus the non-linearity in the resistors conveniently acts to limit the variation in the multiplier compared with the linear result. This is because in the drag-dominated channel, the natural impedance of the channel reduces as turbines are added (due to the dependence of the natural resistance on flow rate), and so the fixed head amplitude driving the channel can do relatively more work on the tidal devices (Cummins, 2013).

For a tidal channel connected to an enclosed bay, the variation in the multiplier γ_B in Equation (8) depends on two parameters: $\lambda_1 = ga_1\delta/(c\omega)^2$ and β (B08). However, as noted in the previous section, B08 have shown that across a realistic range of these parameters, γ_B also varies over a slightly smaller range than the comparative linear result given in Equation (13) (see also Figure 4).

3.1 *Alternative representations of maximum power*

An important observation from the analysis in the preceding section is that the form of the non-linear solution is very similar to that of the linear solution. Motivated by this, new formulations of Equation (4) and Equation (8) can be derived, noting that Equation (11) can be rewritten using standard linear electric circuit theory as:

$$\overline{P}_{max} = \frac{1}{4}\left(\frac{1}{1 + R/|Z|}\right)|I_0|^2|Z|, \tag{14}$$

or

$$\overline{P}_{max} = \frac{1}{4}\left(\frac{1}{1 + R/|Z|}\right)\frac{|V|^2}{|Z|}. \tag{15}$$

These alternative representations of Equation (11) suggest that Equation (4) could be rewritten as:

$$\overline{P}_{max} = \gamma_{GC,2}\rho Q_{0,max}^2\left((c\omega)^2 + \left(\delta Q_{0,max}\right)^2\right)^{1/2}, \tag{16}$$

or

$$\overline{P}_{max} = \gamma_{GC,3}\rho g^2 a_0^2\left((c\omega)^2 + \left(\delta Q_{0,max}\right)^2\right)^{-1/2}. \tag{17}$$

Likewise, Equation (8) could be rewritten as:

$$\overline{P}_{max} = \gamma_{B,2}\rho Q_{0,max}^2\left((c\omega)^2(1-\beta)^2 + \left(\delta Q_{0,max}\right)^2\right)^{1/2}, \tag{18}$$

or

$$\overline{P}_{max} = \gamma_{B,3}\rho g^2 a_1^2\left((c\omega)^2(1-\beta)^2 + \left(\delta Q_{0,max}\right)^2\right)^{-1/2}. \tag{19}$$

Using a similar approach to that given by GC05 and B08, Equation (3) and Equation (7) have been solved numerically to compute $\overline{P}_{max}$. This results has then been compared with the functions in Equations (16) to (19) to calculate the multipliers $\gamma_{GC,2}$, $\gamma_{GC,3}$, $\gamma_{B,2}$ and $\gamma_{B,3}$ (see the Appendix for more information). The solutions for these multipliers are given in Figure 3 and Figure 4 where it can be seen that the different parameters vary over a very similar range to γ_{GC} and γ_B, and can be well approximated for all channel geometries with a value of 0.22. This suggests that the solutions in Equations (16) and (17) are equally convenient alternatives to Equation (4) when $\gamma_{GC} = \gamma_{GC,2} = \gamma_{GC,3}$ =0.22, whilst Equations (18) and (19) are equally convenient alternatives to Equation (8) when $\gamma_B = \gamma_{B,2} = \gamma_{B,3}$ =0.22.

4.0 Simple predictive formulas

4.1 *Maximum power potential*

Following Vennell (2011), if we approximate the geometry of a tidal channel with effective length l_e, cross-sectional area A_e and depth h_e, and adopt a seabed drag coefficient C_d, then (16) to (19) can be rewritten to give simple one-equation predictive formulas for both types of tidal channels.

Firstly, for a channel connecting two large bodies of water we have a set of three equations:

$$\overline{P}_{max} = 0.22\rho g a_0 Q_{0,max}, \tag{20a}$$

$$\overline{P}_{max} = 0.22\rho Q_{0,max}^2 \left(\left(\frac{l_e \omega}{A_e} \right)^2 + Q_{0,max}^2 \left(\frac{C_d l_e}{h_e {A_e}^2} \right)^2 \right)^{1/2}, \tag{20b}$$

and

$$\overline{P}_{max} = 0.22\rho g^2 a_0^2 \left(\left(\frac{l_e \omega}{A_e} \right)^2 + Q_{0,max}^2 \left(\frac{C_d l_e}{h_e {A_e}^2} \right)^2 \right)^{-1/2}. \tag{20c}$$

Likewise, for a channel connected to an enclosed bay we also have a similar set of three equations:

$$\overline{P}_{max} = 0.22\rho g a_1 Q_{0,max}, \tag{21a}$$

$$\overline{P}_{max} = 0.22\rho Q_{max}^2 \left(\left(\frac{l_e \omega}{A_e} \right)^2 (1-\beta)^2 + Q_{0,max}^2 \left(\frac{C_d l_e}{h_e {A_e}^2} \right)^2 \right)^{1/2}, \tag{21b}$$

and

$$\overline{P}_{max} = 0.22\rho g^2 a_1^2 \left(\left(\frac{l_e \omega}{A_e} \right)^2 (1-\beta)^2 + Q_{0,max}^2 \left(\frac{C_d l_e}{h_e {A_e}^2} \right)^2 \right)^{-1/2}, \tag{21c}$$

where

$$\beta = \frac{1}{\omega^2 CL} = \frac{g A_e}{\omega^2 S l_e}. \tag{22}$$

Equations (20a) and (21a) are identical to those given respectively by GC05 and B08, adopting a multiplier of $\gamma_{GC} = \gamma_B$ =0.22, and these equations can be used when the peak undisturbed flow rate and the relevant water amplitude is known. Equations (20b) and (21b) are alternatives to the algorithm presented by Vennell (2011) and can be used when the peak undisturbed flow rate is available, together with an estimate of the channel geometry and seabed drag coefficient. Lastly, Equations (20c) and (21c) are new solutions that can be used when only the difference in water level across the channel, channel geometry, and seabed drag coefficient are known. For this to be the case, an estimate of Q_p is required in both Equation (20c) and (21c), and this can be obtained by ensuring equivalence between all three formulas for each type of channel, so that:

$$Q_{max} = \sqrt{\frac{-\sigma_1^2 + \sigma_1^2\sqrt{1 + \frac{4\left(g a_{a/c}\right)^2}{\sigma_1^4}\sigma_2^2}}{2\sigma_2^2}}. \tag{23}$$

where $\sigma_2 = C_d l_e/(h_e A_e^2)$, $a_{a/c}$ represents the appropriate water level amplitude for each type of channel, and $\sigma_1 = l_e\omega/A_e$, for a Type 1 channel and $\sigma_1 = l_e\omega(1-\beta)/A_e$ for a Type 2 channel.

4.2 *Flow through channel at maximum power potential*

In addition to estimating the power potential it is also important to determine the environmental effects of power extraction. A key metric in this regard is the percentage reduction in flow rate in the channel at maximum power extraction. Adopting the theoretical channel models defined by Equations (3) and (7), we have calculated this numerically in Figure 5 in terms of peak flow rates. It can be seen, as noted by GC05 and Cummins (2013), that the flow is reduced to anywhere between ~50% and ~70% of the undisturbed peak flow rate. Following Cummins (2013), a reasonable first estimate could therefore be taken as 60 % in all cases.

4.3 *Allowing for multiple tidal constituents*

Equations (20) and (21) assume that the tidal channels are forced by a single tidal constituent. GC05 give corrections to include the power due to the additional constituents when multiple tidal constituents are involved. Defining the amplitude of each additional (less dominant) constituent as $a_{0/1,j}$, where j is any integer, these corrections can be given as

$$\bar{P}_{max,corrected} = \bar{P}_{max} \times \left(1 + \frac{\sum a_{0/1,j}^2}{a_{0/1}^2}\right), \quad \text{or} \tag{24a}$$

$$\bar{P}_{max,corrected} = \bar{P}_{max} \times \left(1 + \frac{9}{16}\frac{\sum a_{0/1,j}^2}{a_{0/1}^2}\right), \tag{24b}$$

where $\bar{P}_{max}$ is the original result for one constituent and the subscript $0/1$ implies that the same expressions hold for both types of tidal channel. The first of the corrections, given by Equation (24a), is appropriate when the natural drag in the channel is negligible (i.e. the second term in the brackets of (20b,c) and (21b,c) is a fraction of the first, or the peak flow rate occurs out of phase with the peak dynamic head). The second correction, given by Equation (24b), is appropriate when the natural drag in a tidal channel is much larger than the inertia effect (i.e. the first term in the brackets of (20b,c) and (21b,c) is negligible compared to the second term, or the peak flow rate occurs in phase with the peak dynamic head).

The corrections in Equation (24) can only be applied when the constituents contributing to the dynamic head are known. If these constituent amplitudes are not known (i.e. when using (20b) or (21b)), then they must be calculated. Generally this calculation is complicated, but in the same two special cases accounted for in Equation (24) simple solutions can be obtained. Firstly, for a channel with negligible natural drag, the constituent amplitudes are simply given by the ratio of the flow rate to the channel impedance (ignoring drag):

$$a_{0,j} = \frac{Q_{0,max,j}}{g}\frac{l_e \omega}{A_e}, \quad \text{and} \quad a_{1,j} = \frac{Q_{0,max,j}}{g}\frac{l_e \omega}{A_e}(1-\beta) \tag{25}$$

where $Q_{max,j}$ should be interpreted as the undisturbed amplitude in flow rate for each respective constituent.

Secondly, for the special case of a drag-dominated tidal channel, equations can be written to relate changes in peak flow rate to changes in the tidal amplitude. For example, considering the M2 and S2 tides, the largest peak flow rate $Q_{0,max,S}$ occurs when both constituents are in-phase (i.e. spring tide), whereas the smallest peak flow rate $Q_{0,max,N}$ will occur when they are out-of-phase (i.e. neap tide). Thus the following equations can be written:

$$\rho g(a_{0/1} + a_{0/1,1}) = \rho\left(\frac{C_d l_e}{h_e {A_e}^2}\right)\left(Q_{0,max,S}\right)^2, \tag{26a}$$

$$\rho g(a_{0/1} - a_{0/1,1}) = \rho\left(\frac{C_d l_e}{h_e {A_e}^2}\right)\left(Q_{0,max,N}\right)^2 \tag{26b}$$

The amplitude of the water level elevation associated with the two tidal constituents can therefore be obtained, for either type of channel, by adding and subtracting the above equations:

$$a_{0/1} = \frac{\left(Q_{0,max,S}\right)^2 + \left(Q_{0,max,N}\right)^2}{2g}\left(\frac{C_d l_e}{h_e {A_e}^2}\right), \tag{27a}$$

$$a_{0/1,1} = \frac{\left(Q_{0,max,S}\right)^2 - \left(Q_{0,max,N}\right)^2}{2g}\left(\frac{C_d l_e}{h_e {A_e}^2}\right), \tag{27b}$$

where $a_{0/1}$ is the amplitude of the dominant constituent and $a_{0/1,1}$ is the amplitude of the second constituent.

For any channel that cannot be labelled as having negligible drag, but is not drag dominated, then both Equation (24a) and (24b) could be used, together with Equations (25) and (26) if required, to give an indicative range of power estimates.

5.0 Example calculations

5.1 *Application to existing estimates*

To gauge the performance of the new one-equation formulas presented in Equations (20) and (21) we have applied them to two tidal channels considered previously by Vennell (2011). One is a tidal channel connected to an enclosed bay (Kaipara Harbour). The other is a tidal strait (Cook Strait). For both tidal channels, the complete range of inputs is available so that all three one-equation formulas can be used. The results listed in Table 1 show that there is reasonable agreement between the predictions from all three formulas and the estimates by Vennell (2011). The small variation in results obtained with the different one-equation formulas is due to subjectivity in the choice of channel geometry and drag coefficient, together with errors/uncertainty in the measurement of the dynamic head and flow rate. The slight inconsistencies might also be due to the assumptions of the theoretical model being only approximately correct. Nevertheless, the different approaches appear to give reasonable estimates.

5.2 *Application to the entire Pentland Firth*

As a third example we use the new one-equation formulas to assess the power potential of the Pentland Firth (Figure 6) and compare these results against a recent estimate obtained using a numerical model by Draper *et al.* (2013a). This comparison is also given in Table 1, in which all the input parameters used in each one-equation formulas are listed. Once again the agreement is satisfactory.

The particular inputs in Table 1 for the Pentland Firth were either estimated herein or obtained from the numerical model described by Draper *et al.* (2013a). In practice there will be uncertainty in these inputs, and so a sensitivity analysis (as outlined by Vennell (2011)) is recommended. In particular, in many cases the dimensions of the channel may be very difficult to assess. Likewise, it can be difficult to locate the points for calculation of dynamic head (which should be located in the adjoining sea/ocean representing the large water body or bodies). For these reasons the estimates made with any of the equations given herein should only be treated as initial estimates. More refined estimates can be made through detailed numerical modelling (see, for example, Draper *et al.* (2013a) and Adcock *et al.* (2013)).

6 Discussion

A set of one-equation formulas (Equation (20) and Equation (21)) have been derived that can be used to make rapid assessment of the power potential of tidal channels. The choice of formula depends on which inputs are available (or are easiest to estimate) and the type of channel under consideration. The formulas represent enhancements to existing equations presented by GC05 and B08 and an algorithm presented by Vennell (2011).

The one-equation formulas are based on theoretical models and assumptions introduced by GC05 and B08. Comparison with numerical model predictions suggests that these theoretical models, and their underlying assumptions, are reasonable. However, there is scope to relax some of the model assumptions. For instance, Cummins (2011) has extended B08's model to consider a tidal channel that is sufficiently long for the flow within the channel to be non-divergent. In doing this, Cummins showed that for moderately long channels, turbines should be placed near the mouth of the channel and, if this is achieved, then the estimate from Equations (4) and (8) should be increased by a factor of $1+S_{channel}/S$, where $S_{channel}$ is the surface area of the channel. These corrections can be applied directly to Equation (20) and Equation (21).

Draper (2011) has also extended the model of B08, but in a different way so as to consider an enclosed bay with a surface area S that can vary as the water level in the bay increases and decreases. This is a more realistic assumption for actual bays than that adopted by B08. Using this extended model Draper (2011) showed that whilst the variation in surface area introduces non-linearity into the channel dynamics and an associated asymmetry in the ebb and flood peak flow rate through the channel, Equation (21a) still provides a reasonable estimate of the power potential of a tidal channel, provided the peak undisturbed flow rate used in (21a) is taken as the average of the peak on the flood and ebb tides. This work also suggests that a similar correction should be made when (21b) is used, whilst in both (21a) and (21c) the surface area of the bay should be the still water surface area.

Further extensions to the theoretical models of GC05 and B08 have also been made to account for multiply-connected channels (see Cummins (2013) and Draper et al. (2013b) and the papers cited therein). These extended models can be used as alternatives to those given herein if actual channels cannot be rationalised as a single channel (i.e. if there are two inlets to a single enclosed bay), or if estimates are required for sub-channels within a larger channel.

With or without the extensions noted above, the present formulas could be useful in assessing and ranking different tidal channels for power generation. However, as noted in the introduction, care should be made in any ranking to distinguish between the power potential of a tidal channel and the power which may be extracted economically by tidal turbines within a channel. For instance, if two channels have similar power potential, extraction is more attractive in the tidal channel with the higher peak flow rate (and narrower channel constrictions) because (a) the first turbine installed will see higher flow rates and increased power generation and (b) for a fixed power potential, a high flow rate implies that the natural impedance of the channel is relatively smaller. Given that the power potential is removed when the resistance from turbines matches this impedance, the latter point implies that fewer turbines will be required to remove the power potential when the natural flow rate is higher.

Taking these arguments further, it is easy to see that a channel with high flow rate and low impedance may offer a more economical tidal resource (in terms of power per device) than a channel with lower flow rate, much higher impedance, and possibly a higher power potential. Vennell (2012), building on the theoretical modelling in Vennell (2010), provides a more complete discussion of this topic, including the idealised modelling of tidal turbines; Karsten *et al.* (2012) describe an illustrative comparison of two actual tidal sites.

Nevertheless, despite the need to distinguish between power potential and economic power generation when ranking different channels, the one-equation formulas presented herein are a useful first step in any resource assessment. In particular, they present insight into the channel dynamics (relative flow rates, impedance and dynamic head) which leads to more detailed estimates of the resource and has implications for metrics such as power per tidal device. The formulas are also useful for cross-validation with numerical models and in providing an estimate of the upper bound to power generation from a tidal channel.

Acknowledgements

The first author gratefully acknowledges the support of the Lloyd's Register Foundation. Lloyd’s Register Foundation invests in science, engineering and technology for public benefit, worldwide.

References

Adcock, T. A. A., Draper, S., Houlsby, G. T., Borthwick, A. G. L., and Serhadlioglu, S. (2013), “The available power from tidal stream turbines in the Pentland Firth”, Proceedings of the Royal Society, Part A, 469:20130072.

Blanchfield, J., Garrett, C., Wild, P. and Rowe, A. (2008), “The extractable power from a channel linking a bay to the open ocean”, Proc. Inst. Mech. Engineers, Part A: J. Power and Energy, 222, pp. 289-297.

Black & Veatch (2005) ‘Phase II: UK tidal stream energy resource assessment’. Carbon Trust Marine Energy Challenge, 2005

Cummins, P.F. (2013), “The extractable power from a split tidal channel: An equivalent circuit analysis”, Renewable Energy, 50, pp. 395-401.

Cummins, P.F. (2011), “On the extractable power from a tidal channel”, J. Waterway, Port, Coastal, Ocean Eng., 138, pp. 63-71.

Draper, S., Adcock, T. A. A., Borthwick, A. G. L. and Houlsby, G. T. (2013a) “Estimate of the Extractable Pentland Firth Tidal Stream Power Resource”, submitted Renewable Energy.

Draper, S., Adcock, T.A.A., Borthwick, A.G.L. and Houlsby, G.T. (2013b) “An Electrical Analogy for the Pentland Firth Tidal Stream Power Resource”, submitted to Proceedings of the Royal Society, Part A.

Draper, S., (2011), “Tidal stream energy extraction in coastal basins”, DPhil Thesis, University of Oxford, U.K.

Garrett, C. & Cummins, P. (2005), “The power potential of tidal currents in channels”. Proceedings of the Royal Society London A, 461, pp.2563-2572.

Garrett, C. & Cummins, P. (2004), “Generating Power from Tidal Currents”, J. Waterway, Port, Coastal, Ocean Eng., 130, pp. 114-118.

Karsten, R.H., McMillan, J.M., Lickley, M.J. and Haynes, R.D., (2008), “Assessment of tidal current energy in the Minas Passage, Bay of Fundy Proceedings of the Institution of Mechanical Engineers, Part A: Journal of Power and Energy (222), pp. 493-507.

Karsten, R.H., O’Flaherty-Sproul, M., McMillan, J., Culina, J., Trowse, G. and Hay, A. (2012) “Analysis of Tidal Turbine Arrays in Digby Gut and Petit Passage, Nova Scotia”, 4th International Conference on Ocean Energy. Dublin, Ireland.

Sutherland, G., Foreman, M. & Garrett, C., (2007), “Tidal current energy assessment for Johnstone Strait, Vancouver Island.” Proceedings of the Institution of Mechanical Engineers, Part A: Journal of Power and Energy, 221(2), pp. 147–157.

Triton Consultants Ltd. (2006), “Canada Ocean Energy Atlas (Phase 1) potential tidal current energy resource analysis background”. Prepared for the Canadian Hydraulics Centre, Natural Resources Canada.

Vennell, R. (1998), “Oscillating Barotropic Currents along Short Channels”, Journal of Physical Oceanography, 28, pp.1561-1569.

Vennell, R. (2010), “Tuning turbines in a tidal channel.” Journal of Fluid Mechanics, 663, 253-267.

Vennell, R. (2011), “Estimating the Power Potential of Tidal Currents and the Impact of Power Extraction on Flow Speeds”, Renewable Energy, 36, pp. 3558-3565.

Vennell, R. (2012), “The Energetics of Large Tidal Turbine Arrays”, Renewable Energy 46, 210 – 219.

Appendix

We now explain how the multipliers in Equations (16) to (19) were obtained. Starting with the case of a channel connected to an enclosed bay, Equation (7) is rewritten as the following system of first order differential equations (see also B08):

$$\frac{d\xi_b}{dt} = \frac{Q}{S}, \tag{A1}$$

and

$$\rho c \frac{dQ}{dt} = \rho g \xi_c - \rho g \xi_b - (\rho\delta|Q| + \rho\delta_1|Q|)Q. \tag{A2}$$

Introducing the non-dimensional variables $Q = Q' g a_c/(c\omega)$, $(\xi_c, \xi_b) = (\xi_c', \xi_b')a_c$, $t = t'\omega^{-1}$ and $(\delta_t, \delta) = (\lambda_t, \lambda_1)(c\omega)^2/(ga_c)$, these equations can be then be rewritten as:

$$\frac{d\xi_b'}{dt'} = \beta Q', \tag{A3}$$

and

$$\frac{dQ'}{dt'} = \cos(t') - \xi_b' - (\lambda_t + \lambda_1)|Q'|Q'. \tag{A4}$$

where $\xi_c = a_c \cos(\omega t)$. Equations (A3) and (A4) show that the flow through the channel is dependent on just three parameters: λ_1, λ_t and β. Searching for the maximum power, the optimum value of λ_t is therefore solely a function of λ_1 and β (B08). Equations (A3) and (A4) are solved herein using a Runge Kutta time-stepping scheme (starting from initial conditions $\xi_b' = Q' = 0$) for a particular value of λ_1 and β, for a range of values of the parameter λ_t to search for the peak value in the non-dimensional power:

$$\overline{P}' = \lambda_t \overline{|Q'|^3}. \tag{A5}$$

Writing this maximum as $\overline{P}'_{max}$, the values of the relevant multipliers are then computed as:

$$\gamma_B = \frac{\overline{P}'_{max}}{Q'_{max}}, \tag{A6}$$

$$\gamma_{B,2} = \frac{\overline{P}'_{max}}{(Q'_{max})^2[(1-\beta)^2 + (\lambda_1 Q_0')^2]^{\frac{1}{2}}}, \tag{A7}$$

and

$$\gamma_{B,3} = \frac{\overline{P}'_{max}}{[(1-\beta)^2 + (\lambda_1 Q'_{max})^2]^{-\frac{1}{2}}}, \tag{A8}$$

where Q'_{max} is the peak non-dimensional flow rate computed for the given value of λ_1 and β when $\lambda_t = 0$.

For the case of a tidal channel connected to two large water bodies, the solutions follow in the same way as above, except that $\beta = 0$ and a_c is now equivalent to a_a and λ_1 becomes λ. We therefore calculate the multipliers for a tidal channel connected to two large water bodies in the same way as outlined above (and using the same numerical code), but with β =0.01 (i.e. with β =0.01 we let $\gamma_{GC} = \gamma_B$, $\gamma_{GC,2} = \gamma_{B,2}$ and $\gamma_{GC,3} = \gamma_{B,3}$).

Figures

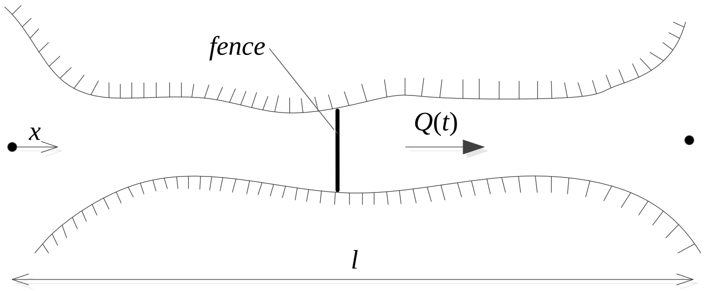

(a)

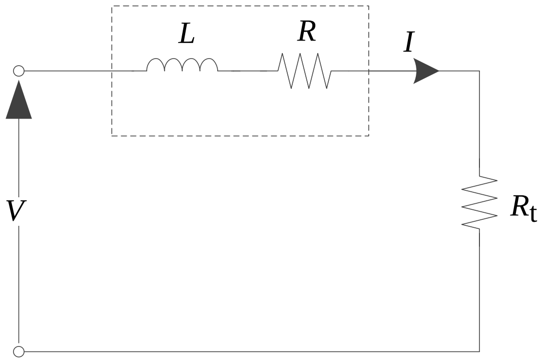

(b)

Figure 1: (a) Single tidal channel connecting two large bodies of water. (b) Equivalent electric circuit. Dashed box highlights the natural channel elements.

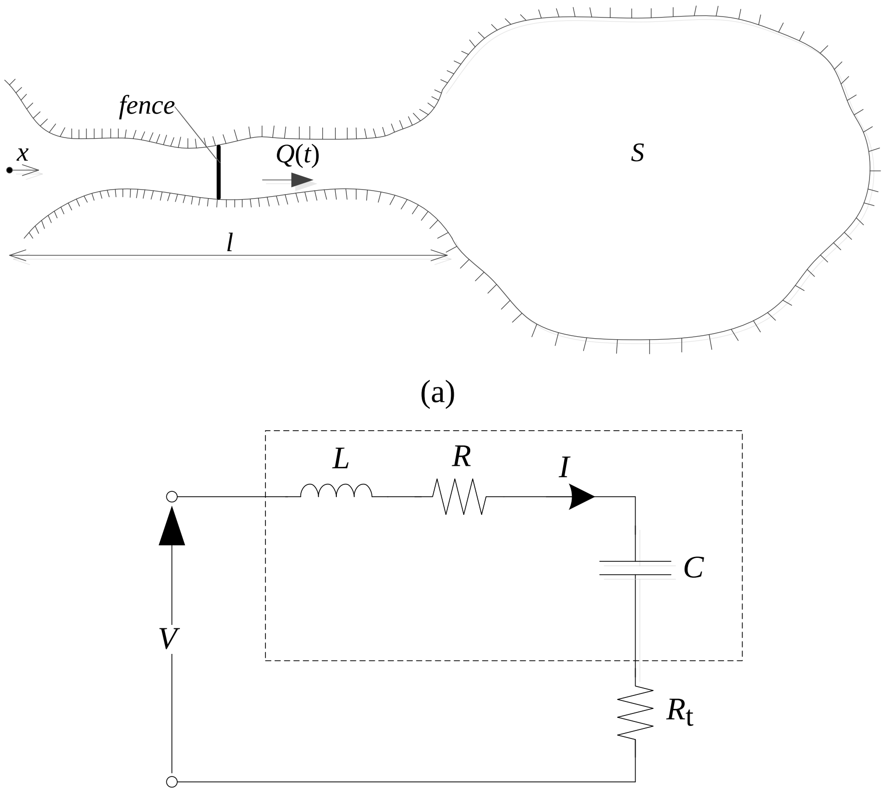

(a)

(b)

Figure 2: (a) Single tidal channel connecting an enclosed bay to the open sea. (b) Equivalent electric circuit. Dashed box highlights the natural channel elements.

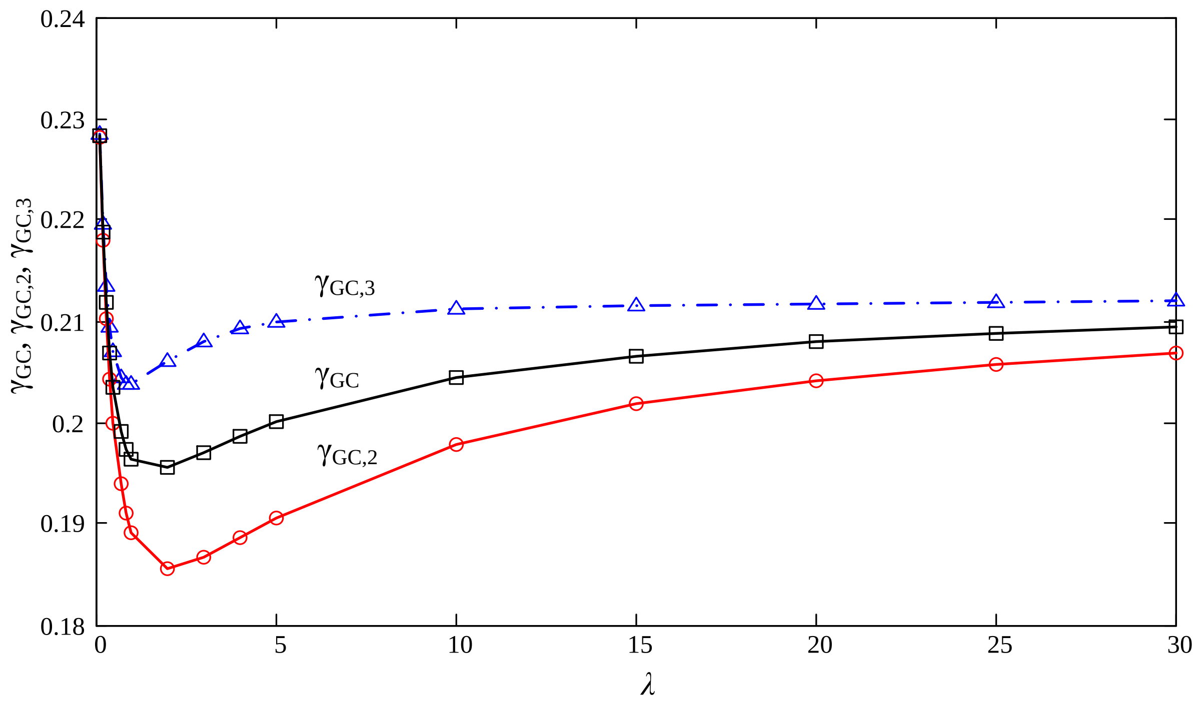

Figure 3: Variation in the multipliers γ_{GC}, $\gamma_{GC,2}$ and $\gamma_{GC,3}$ as a function of the dimensionless parameter $\lambda = g a_a \delta/(c\omega)^2$. Markers indicate discrete values computed numerically.

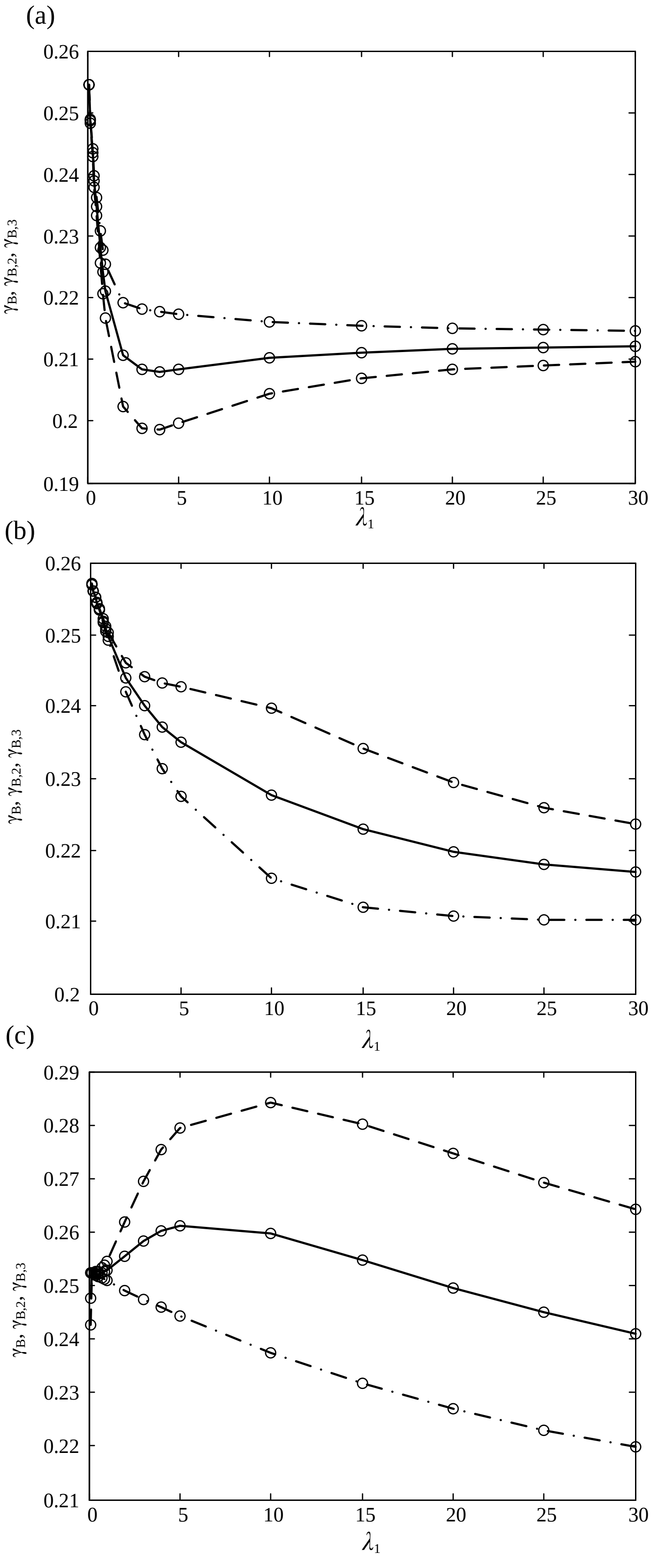

Figure 4: Variation in the multipliers γ_B (solid line), $\gamma_{B,2}$ (dashed line) and $\gamma_{B,3}$ (dash-dot line) as a function of the dimensionless parameter $\lambda_1 = ga_c\delta/(c\omega)^2$; (a) β =2, (b) β =5, and (c) β =10. Circle markers indicate discrete values computed numerically.

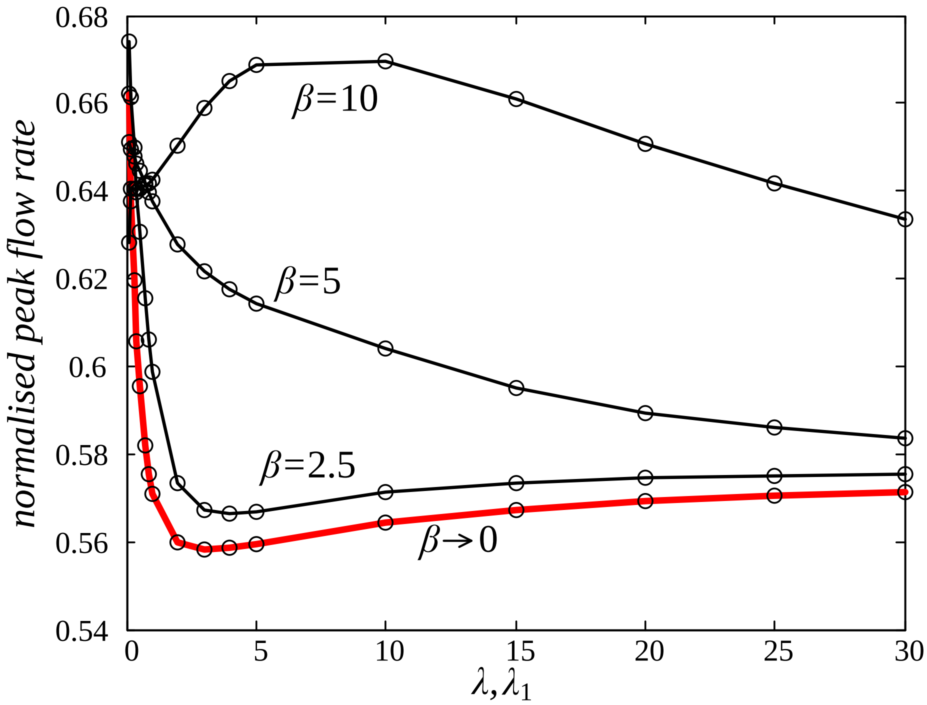

Figure 5: Peak flow rate in a tidal channel when turbines extract maximum power, normalised by peak natural flow rate. Circle markers indicate discrete values computed numerically.

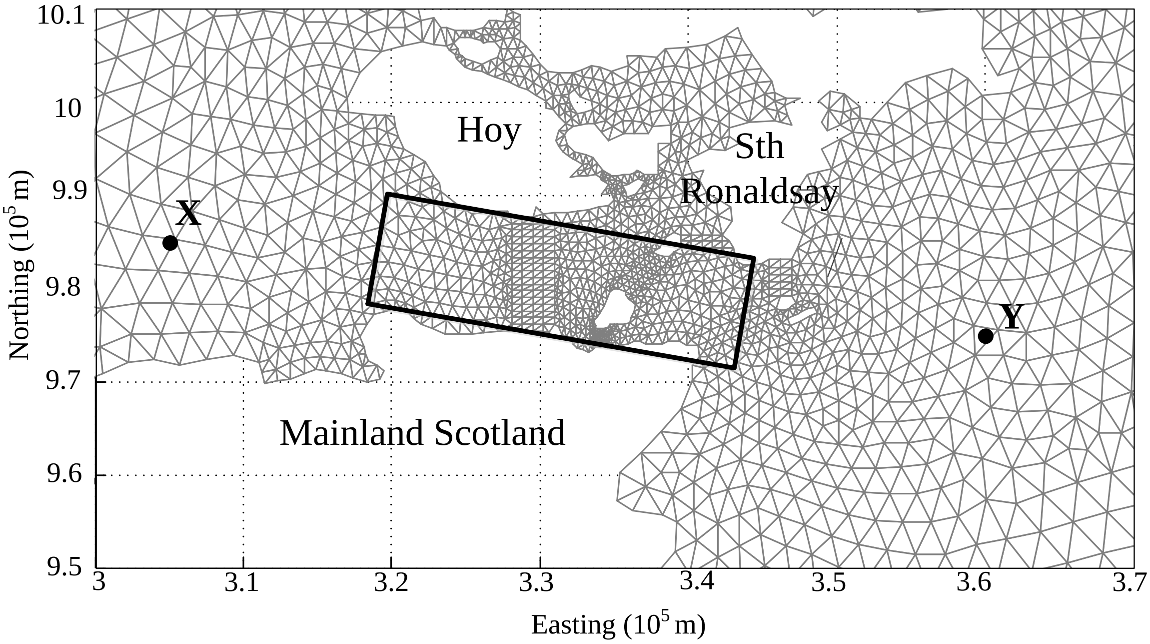

Figure 6: The Pentland Firth, UK. Numerical mesh used to simulate tidal flows (see Draper *et al.* (2013a) for more details). The black box has length and width given in Table 1 and is an approximate representation of the geometry of the tidal channel. The amplitude of water level difference across the channel (listed as a_a in Table 1) is calculated between points X and Y.

Tables

	Units	Cook Strait	Kaipara Harbour	Pentland Firth
General Inputs				
Dominant tidal frequency, ω	rad/s	0.000141	0.000141	0.000141
Water density	kg/m^3	1025	1025	1025
(i) Water elevation				
Elevation difference ($a_{a/c}$)	m	1.6	1.05	1.32*
(ii) Peak flow rate				
Peak undisturbed flow rate	SV	4.4	0.11	1.17*
Estimate of σ_1 for Equation (23)	rad/m.s	3.7E-06	-8.6E-05	7.8E-06
Estimate of σ_2 for Equation (23)	m^{-4}	1.2E-13	3.8E-10	5.1E-12
Peak undisturbed flow rate; Equation (23)	SV	4.2	0.11	1.3
(iii) Channel Geometry and seabed drag				
Channel Length, l_e	km	100	15	25
Channel Depth, h_e	m	150	25	60
Channel Width	km	25	2.5	7.5
Cross-sectional Area, A	km^2	3.75	0.0625	0.45
Mean bay surface area, S	km^2	NA	580	NA
Seabed drag coefficient, C_d	-	0.0025	0.0025	0.0025*
β	-	NA	3.56	NA
Estimate of Power potential				
Vennell (2011)	GW	15	0.24	-
Draper et al. (2013)	GW	-	-	3.8
Equation (20a) and (21a)	GW	15.6	0.26	3.4
Equation (20b) and (21b)	GW	16.5	0.26	3.0
Equation (20c) and (21c)	GW	14.7	0.25	3.7

Table 1: Predictions using Equation (20) for Cook Strait, New Zealand, and Equation (21) for Kaipara Harbour. Input data for these locations are from Vennell (2011). Also shown are predictions for Pentland Firth, UK. Input data marked with '*' from Draper *et al.* (2013) for the Pentland Firth, remaining data estimated. Note, the estimates from Equations (20c) and (21c) use the peak undisturbed flow rate computed from Equation (23).